Wave Dependence of Sea-Surface Wind Stress

YOSHIAKI TOBA

Department of Geophysics, Faculty of Science, Tohoku University, Sendai, Japan

NORIKO IIDA

National Center for Science Information System, Tokyo, Japan

HIROSHI KAWAMURA AND NAOTO EBUCHI

Department of Geophysics, Faculty of Science, Tohoku University, Sendai, Japan

IAN S. F. JONES

Marine Studies Centre, The University of Sydney, N.S.W., Australia

(Manuscript received 8 December 1988, in final form 9 November 1989)

ABSTRACT

Distribution of the wind stress over the oceans is usually estimated by using a bulk formula. It contains the squared 10-m wind speed multiplied by the drag coefficient, which has been assumed in many cases to be a weak function of the 10-m wind speed. Over land the important role of thermal stratification has been clearly recognized, but over the sea the influence of wind waves is less well documented. This paper presents evidence showing the likelihood that the influence of the wind waves can also be large. Charnock proposed an expression for the marine atmospheric boundary layer roughness parameter, z_0, which depended only on the wind friction velocity, u_*, and the acceleration of gravity, g. Toba and Koga have recently proposed an alternative expression for flow over growing wind waves, which are in local equilibrium with the wind, given by a form including the wind-wave spectral peak frequency explicity. The criterion for local equilibrium of the wave field with the wind is its consistency with the $^3/_2$-power law between nondimensional wave height and wave period normalized by u_* and g. The differences between these expressions are significant. The two expressions are compared with a composite dataset which comprises some representative data from laboratories and tower stations together with data from storms at an oil producing platform in Bass Strait, Australia. In these storms strong winds up to 25 m s^{-1} and large wind waves up to 12 s in significant wave period, from a direction of long fetch, lasted for two or three days. The composite dataset shows that the drag coefficient C_D depends also on the sea state and that in storm conditions C_D can be larger by a factor of two to three than the value that Charnock's expression usually predicts. Further experiments focussing on the examination of the effect of ocean waves on the wind stress are recommended.

1. Introduction

The accurate estimate of the distribution of air–sea fluxes of momentum, heat, water vapor and other gasses, is a very important issue in developing coupled ocean–atmosphere models. However, there seems to be considerable disagreement among authors of the best manner in which to parameterize the fluxes in terms of the bulk properties of the atmosphere and ocean. This problem is also important for satellite sensing of the global wind field.

Air–sea fluxes have frequently been estimated by using bulk transfer coefficients; for momentum it is called the drag coefficient C_D. Over land the role of thermal stratification has been clearly recognized (e.g., Kondo 1975). Over the sea, the value of C_D, which is expressed traditionally as a function of the 10-m wind speed U_{10}, has been given in various formulas as summarized in Fig. 1 of Blanc (1985). One cause of disagreement among the observed data and these various expressions lies in the difficulty of measuring the stress values over the ocean. However, another cause is the poor parameterization of the effect that wind waves can have on fluxes. Because of the difficulty of flux measurement under conditions of large wind waves and strong winds, available data for these conditions are very few.

Charnock (1955) proposed, from a dimensional argument, his well known formula:

$$gz_0/u_*^2 = \beta, \tag{1}$$

Corresponding author address: Prof. Yoshiaki Toba, Department of Geophysics, Faculty of Science, Tohoku University, Sendai 980, Japan.

where z_0 is the roughness length, u_* the friction velocity of air, and g the acceleration of gravity, with β as a numerical constant. For the value of β, Smith and Banke (1975) proposed 0.0130, while Garratt (1977) suggested 0.0144. Wu (1980) from a review of many experiments proposed $\beta = 0.0185$ a value which corresponds approximately to the expression for the drag coefficient,

$$C_D = (0.80 + 0.065\ U_{10}) \times 10^{-3} \qquad (2)$$

with U_{10} in m s^{-1}. Equations (1) and (2) predict the wind stress on the assumption that the features of the wind waves relevant to z_0 are already adequately parameterized by the wind stress itself.

On the other hand, several efforts have been made to incorporate the effect of wind waves more explicitly. Various physical mechanisms for the wind stress to depend on the underlying wave field have been proposed. Kitaigorodskii and Volkov (1965), Volkov (1970), Kitaigorodskii and Zaslavsky (1974) introduced the wave age (C/u_*) into parameters influencing z_0, C is the phase speed of wave components and the parameter is in the form of weighting function with emphasis on short wave components. Toba and Kunishi (1970) demonstrated the association between wind-wave breaking and an increase of the wind stress. Banner and Melville (1976) also reported that wave breaking enhanced the shear stress. Melville (1977) tried to use quantities related with wave breaking conditions in the expression of roughness length. Kondo et al. (1973) postulated that the roughness is essentially supported by ripples of the angular frequency 10–200 rad s^{-1}. Wu (1986, 1988) considered the differential contributions to the wind stress of short-wave roughness elements and the momentum flux going directly to long waves, and asserted that the former is the primary contribution to the Charnock expression.

Toba (1979), Toba and Koga (1986) proposed, from dimensional considerations combined with data analyses, another expression for z_0 incorporating the angular frequency of wind-wave spectral peak, σ_p, as

$$z_0\sigma_p/u_* = \gamma, \quad \gamma = 0.025. \qquad (3)$$

Since Eq. (3) was also expressed as

$$gz_0/u_*^2 = \gamma C_p/u_*, \qquad (3a)$$

where C_p is the phase speed of waves of the spectral peak frequently, this corresponds to the simplest case of Stewart's (1974) general expression for z_0:

$$gz_0/u_*^2 = f(C_p/u_*). \qquad (4)$$

It should be noted that Eq. (3) is proposed for wind waves which are growing in "local equilibrium with the wind."

The form of Eq. (3) requires that z_0 depend strongly on the stage of development of the wind waves. Since we are concerned with the local equilibrium waves, as we will see below, the period, wave height and wind stress are related. If z_0 is converted to the equivalent drag coefficient C_D, an example of winds of 20 m s^{-1} and significant wave period of 10 s, gives the values of air–sea transfer of momentum three times larger than that usually assumed by expressions such as Charnock's. Boyle et al. (1987) reported, as a result of measurements based on the turbulent kinetic energy dissipation rate, that the bulk method with the usual drag coefficient values underestimated the stress by as much as a factor of three in storm conditions, while the estimates were quite good in meteorological conditions free of surface storms, troughs and ridges.

Brutsaert and Toba (1986) provided a rationale for this expression Eq. (3) by analogy to solid surfaces, by noting that $z_0 = H_s f(\delta)$ where δ is the steepness of the ocean waves. However, they deduced Eq. (3) with the aid of the $^3/_2$-power law and an effective dispersion relationship in which particular characteristics of wind waves are already included. We should not strictly interpret this as that the physical process of the sea-surface drag is equivalent to the drag over solid surfaces having the same H_s and δ as those of ocean waves. The real drag is the synthesis of momentum transfers from the air to the sea state which consists of all the components of the individual waves of a continuous spectrum. The peak frequency σ_p enters as a measure of the whole of the wind-wave frequency spectral range over which the momentum transfer processes are occurring. Also it is not proposed to use σ_p in conditions where $C_p/U_{10} \gg 1$ as such waves are not in local equilibrium with the wind. Remotely generated swells fall into the latter category.

Volkov (1970), Donelan (1982), Geernaert et al. (1987), however, have proposed an influence of wind waves that had just the opposite effect, with decreasing drag coefficient with increasing wave age. As well, Masuda and Kusaba (1987) presented laboratory data which supported a dependence on σ_p that was the reciprocal to that of Eq. (3). The functional form of Eq. (4) is still considered undetermined (Wu 1988).

In order to examine whether a developed wind-wave field enhances the wind stress over Charnock's expression, diminishes it or is not important, we should use data that includes large wind waves, with a significant wave period, T_s, of the order of 10 s forced by strong winds. However, the lack of good quality data from the hostile environment of the open ocean under large seas inhibits convincing tests of the above concepts.

The present paper proposes a new way of extracting the wind stress for such severe conditions, from routinely observable variables such as the wind speed at a given level, significant wave height and period of wind waves. It invokes the $^3/_2$-power law (Toba 1972, 1978) for wind waves which are in local equilibrium with the wind. We have available a good set of wind speed, wave height and period measurements obtained during storms from an oil producing platform in Bass Strait,

Australia to test this idea. The results provide evidence that the influence of the wind waves can be important. The data used here are for two storms at one observation site. It is an ideal site with large fetches and deep water. We propose that similar tests be attempted at various other observation sites.

Since we use the $^3/_2$-power law for the stress estimates, we review briefly, in section 2, the robustness of this relation, including the validity of the value assumed for the numerical constant. In section 3 the description of the Bass Strait data is given, and the selection of local equilibrium wave data is made for the comparison test of z_0 formulas by Charnock and by Toba and Koga in section 4. Then in section 5, we look at the air–sea interaction balances, the potential errors in the above approach, and propose some possible expressions for the wave dependence of sea surface wind stress.

2. A review of the $^3/_2$-power law

The $^3/_2$-power law was proposed by Toba (1972) for growing wind waves, and was expressed as

$$H^* = BT^{*3/2}, \quad B = 0.062, \tag{5}$$

or in the dimensional form,

$$H_s = B(gu_*)^{1/2}T_s^{3/2}, \quad B = 0.062, \tag{5a}$$

where $H^* = gH_s/u_*^2$ is the nondimensional wave height, $T^* = gT_s/u_*$ the nondimensional period, T_s being the significant wave period. This power law was originally proposed after examination of empirical formulas for the growth of wind waves by Wilson (1965), Mitsuyasu et al. (1971) and experimental data by Toba (1961). We will reexamine the robustness of the numerical value of B in Eq. (5a).

The Wilson's formula is a set of

$$\hat{H} = 0.30[1 - (1 + 0.004\hat{F}^{1/2})^{-2}] \tag{6a}$$

$$\hat{T} = 1.37[1 - (1 + 0.008\hat{F}^{1/3})^{-5}] \tag{6b}$$

where $\hat{H} = gH_s/U_{10}^2$, $\hat{T} = gT_s/2\pi U_{10}$, $\hat{F} = gF/U_{10}^2$ and F is the fetch. For short fetches (6a) and (6b) were reduced to simple formulas of

$$\hat{H} = 0.0024\hat{F}^{1/2} \tag{7a}$$

$$\hat{T} = 0.0548\hat{F}^{1/3} \tag{7b}$$

respectively, showing

$$\hat{H} \propto \hat{T}^{3/2} \tag{8}$$

by elimination of the nondimensional fetch $\hat{F}$. Equations (6a) and (6b) express the asymptotic approach of $\hat{H}$ and $\hat{T}$ to saturation values of 0.30 and 1.37, respectively. In spite of the complicated forms of (6a) and (6b), if we eliminate $\hat{F}$, the relation (8) holds substantially for the whole region of $\hat{F}$, as reported by Toba (1972). The JONSWAP formula by Hasselmann et al. (1973):

$$\hat{E} = 1.6 \times 10^{-7}\hat{F} \tag{9a}$$

$$\hat{f}_p = 3.5\hat{F}^{-0.33}, \tag{9b}$$

where $\hat{E} = g^2E/U_{10}^4 = \hat{H}_s^2/16$, $\hat{f}_p = U_{10}f_p/g$, f_p is the peak frequency, and also the Mitsuyasu et al. (1971) formula

$$\hat{H} = 2.15 \times 10^{-3}\hat{F}^{0.504} \tag{10a}$$

$$\hat{T} = 5.07 \times 10^{-2}\hat{F}^{0.330} \tag{10b}$$

give essentially the same relation. Toba (1972) considered that in wind waves H_s and T_s are not independent but are always related to each other under the action of wind. This state of equilibrium is maintained by strongly nonlinear processes in the wind–wind wave dynamics, and its characteristic value, as expressed by $\hat{H}$ or by $\hat{T}$, evolves slowly with the fetch or the duration. Toba called such an equilibrium state "the local balance (equilibrium) in the air–sea boundary processes." This concept has been investigated intensively by wind–wave tank experiments (as reviewed by Toba 1985), and a further discussion was also given (Toba 1988).

Though the empirical formulas Eqs. (6a) to (10b) were given in forms normalized by U_{10}, the physical processes should be related to u_*, the friction velocity. Thus, Toba (1972) expressed the relation of Eq. (8) as Eq. (5) by using H^* and T^* normalized by u_*. However, a conversion from U_{10} to u_* needs an average value of C_D weighted by frequency of occurrence, or an "overall value" of C_D, since by definition of C_D,

$$u_* = (C_D)^{1/2}U_{10}. \tag{11}$$

The adoption of differing values of the overall C_D causes a variation of B. Figure 1 shows the relation between the overall C_D and B which is consistent with the above wave-growth formulas. For the usually measured range

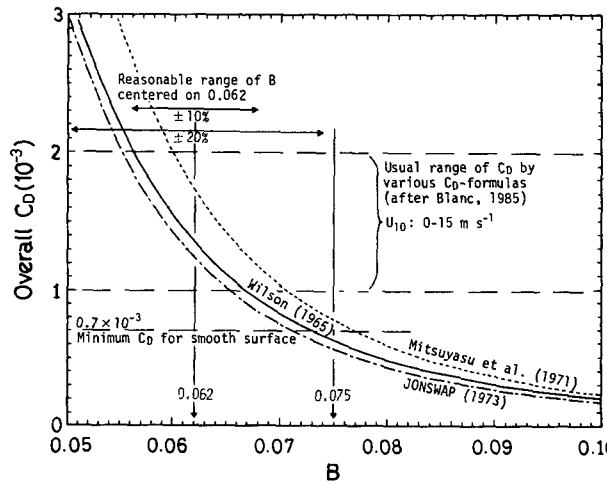

FIG. 1. Relation between the overall C_D and B in Eq. (5) or (5a), such as consistent with wind-wave growth formulas.

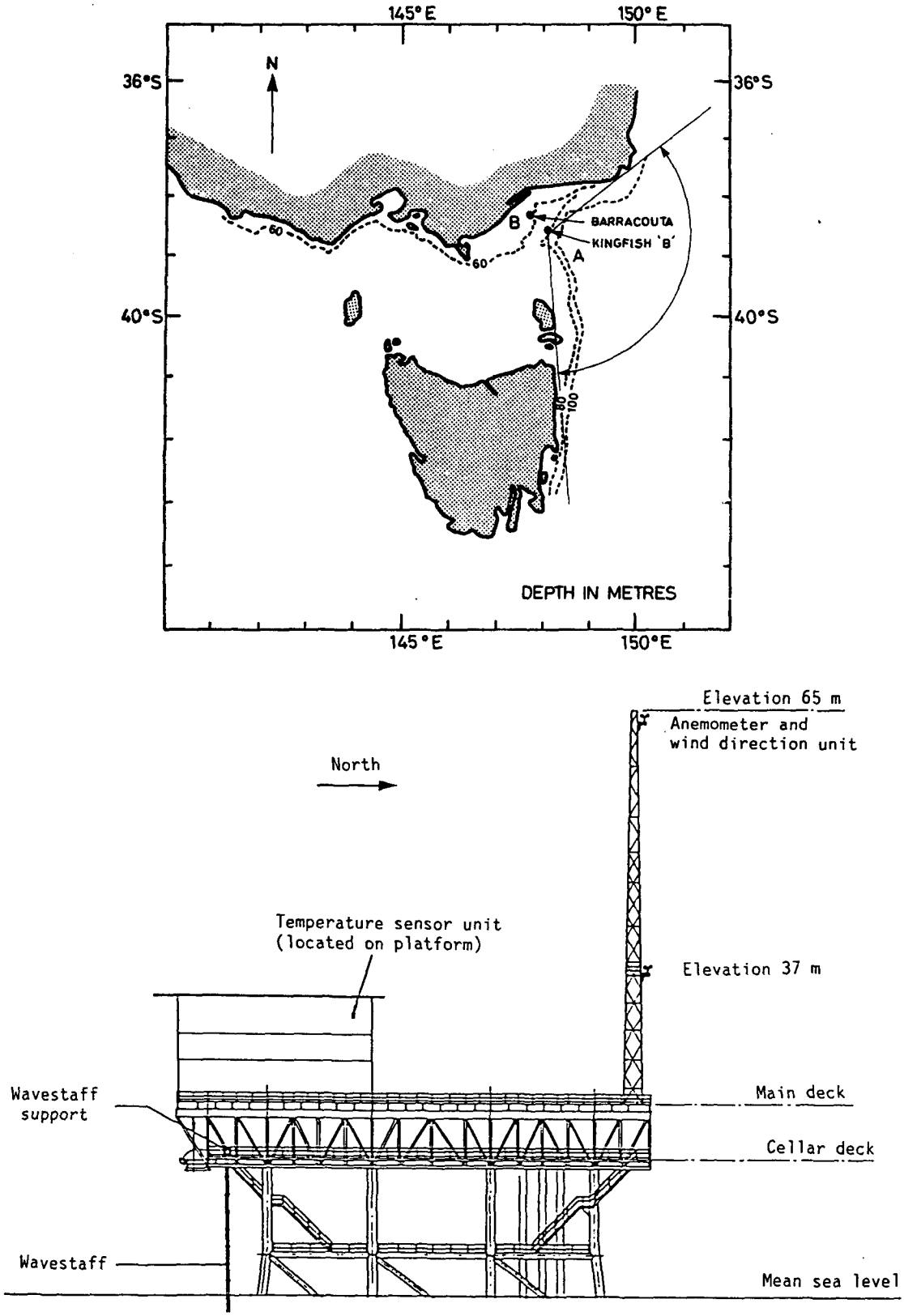

FIG. 2. Location of the oil-production platform Kingfish B in Bass Strait, Australia, and a sketch of the platform with positions of the observation sensors.

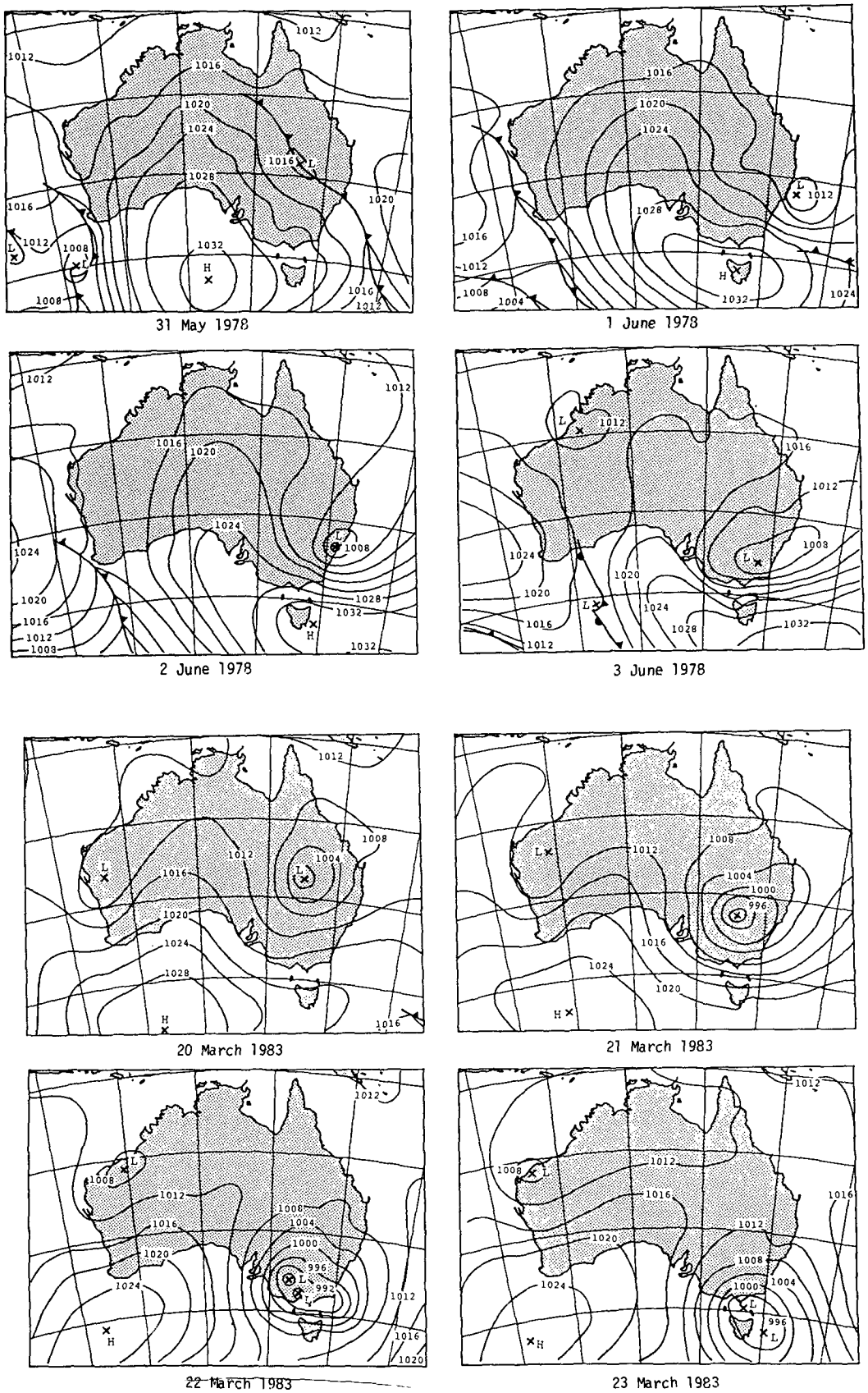

FIG. 3. Weather maps for two storms: STM24 of May 1978 and STM212 of March 1983.

of C_D of (1.0–2.0) $\times 10^{-3}$ for U_{10} of 0–15 m s^{-1}, as reviewed by Blanc (1985), a reasonable range of the B-value is considered to be 0.062 ± 10%. In later part of this article we propose larger values of C_D for severe sea conditions. However, since the curves of Fig. 1 are very steep for the left side part of the figure, the variation of C_D in this part does not so greatly affect the value of B. Moreover, the frequency of occurrence of these large C_D conditions is not large. Consequently, it is reasonable to assume the above-described range of B.

Later in section 4 in Figs. 9 and 10, we will show other data available from Kawai et al. (1977), Donelan (1979), Merzi and Graf (1985), in which u_* was measured. These data points are also distributed centered on 0.062.

This similarity law (5a) has been used effectively in wave prediction models such as the TOHOKU Wave Model (Toba et al. 1985). Toba (1988) argues that the state of local equilibrium as expressed by (5a) is brought about by the "breaking adjustment of wind waves" which is required by the continuity of velocity and momentum flux across the air–water boundary. It should be noted that this power law is satisfied by a wide range of wind waves from laboratory tanks to fully-developed saturation conditions in the ocean, though it is not satisfied for waves if the wind speed decreases quickly so that $C_p/U_{10} \gg 1$, or for swells which have propagated from remote regions. The present paper confines itself to the problem of pure wind waves which are in local equilibrium with the wind, defined as satisfying the similarity law (5a).

3. Bass Strait data

a. The selection of local equilibrium wave data

The data which have been used for the present study were obtained at an ESSO oil producing platform, Kingfish B, in the eastern part of Bass Strait, Australia. The water depth of Kingfish B is 77 m, and it becomes deeper in the easterly direction that is open to the Tasman Sea. Figure 2 shows the location of the platform in the Bass Strait, and a sketch of the platform with positions of the observation sensors. A description of the data acquisition system may be found in Bailey et al. (1989). It used a Baylor wave gauge and digital recording to produce wave and wind statistics. Some discussion of the consequence of measurement errors will also be given at the end of section 4.

We have selected two storms from the wind and wave data compiled by Jones and Toba (1985): STM24 of May 1978 and STM212 of March 1983. In these storms, strong winds from 10 to 25 m s^{-1}, and large wind waves from 6 to 12 s in significant wave period T_s from the east and southeast (long fetch directions) lasted for three (STM212) or two (STM24) days. Figure 3 shows the weather maps for these storms. (In Jones and Toba (1985), data of another storm, STM95, was given. However, we excluded this case in the present analysis since the wind was from the northwest and we are not confident that the wave gauge was not in the wake of the platform for some period of this storm.)

The data comprise wind speed U_{37} at 37 m (STM24) or U_{65} at 65 m (STM212), the significant wave height H_s and the zero-crossing average wave period $\bar{T}$, which were derived from records 1024 seconds long taken at intervals of 20 minutes. As for conversion from $\bar{T}$ to T_s and σ_p, we use

$$T_s = A\bar{T}, \quad A = 1.13. \tag{12}$$

The value of $A = 1.13$ has been chosen since this was the average value of 132 detailed time series from STM212. Since the factor A has a significant effect upon the results as discussed later, it is much better to use T_s if it is available. But this time only the time series of $\bar{T}$ is available. As for conversion from T_s to σ_p, we use

$$\sigma_p = 2\pi/1.05T_s \tag{13}$$

after both Mitsuyasu (1968) and Toba (1973). Figures 4 and 5 show the time series of the wind speed and direction. Figure 6 shows the time series of T_s.

Together with the similarity law expressed by Eq. (5a), we also assume the logarithmic wind profile:

$$U(z)/u_* = (1/\kappa)\ln(z/z_0) \tag{14}$$

to estimate z_0, where $U(z)$ is the wind speed at a level z and κ (=0.40) is the von Kármán constant. If there is thermal stratification in the air boundary layer, (14)

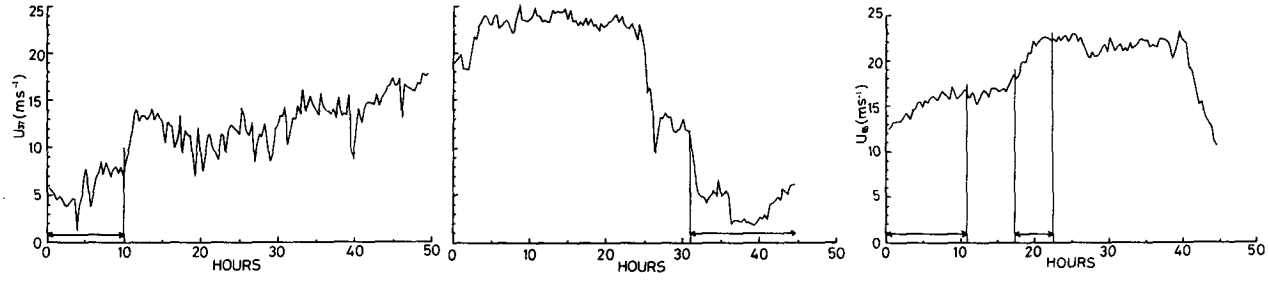

FIG. 4. Time series of wind speed. The left and the middle panels are for STM24, and the righ panel is for STM212. The left panel starts (local time) at 0717 31 May, ends at 0917 2 June 1978, the middle starts at 1410 2 June, ends at 2151 4 June 1978 with short intermissions at 12.3 h and at 36.3 h, the right panel starts at 1217 20 March and ends at 0834 22 March 1983. The periods with horizontal arrows were excluded in the latter analyses beginning at Fig. 9.

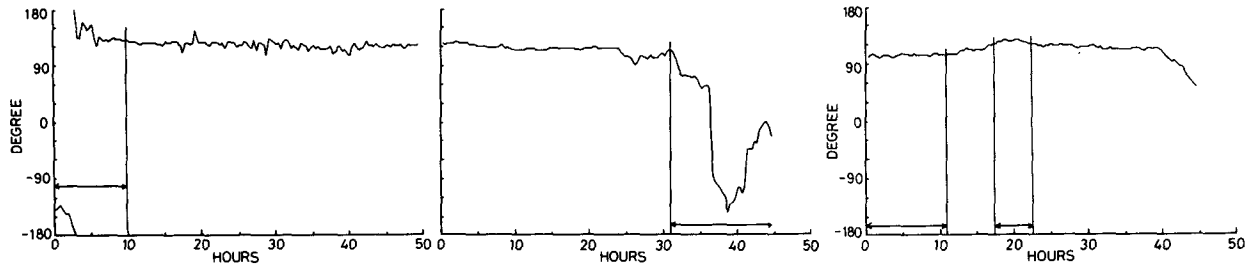

FIG. 5. Time series of wind direction. Panels as in Fig. 4.

should be modified, especially for weak winds. However, we selected examples of strong average winds (10–25 m s^{-1} in the case of STM24, and 17–23 m s^{-1} in STM212) from directions of very large fetches from the east. The observed air temperature measured at 30 m ranged between 12° and 18°C in STM24 and between 19° and 20°C in STM212, with the surface water temperature from climatology average of 16° and 20°C for these periods, respectively (Jones 1980). Consequently, we can assume that the thermal stratification was near neutral and within the criterion we discuss later. There is no data of humidity at the observation site. However, since the wind speed was large, the effect of humidity on the momentum flux estimates from wind profiles can be considered negligible (cf. Blanc 1983).

First we wish to determine those periods where the Bass Strait waves satisfy local equilibrium. We have two expressions for z_0: Eq. (1) and Eq. (3). We combine these with Eq. (14) and the time series of $U(z)$ to obtain two series of u_* by iteration. With these two series of u_* together with the data of T_s, we obtain two series of H_s by using the $^3/_2$-power law (5a) in order to compare these predictions with the measured wave heights. We name the values of wave height thus calulated H_{sc1} and H_{sc2}. Figure 7 shows H_{sc1} (dotted line) calculated from Eq. (3) together with the observed H_s (thick line). At most times the two curves agree with each other. Figure 8 shows H_{sc2} (thin line) calculated from Eq. (1) together with the observed H_s (thick line). In Fig. 8 the curve of H_{sc2} is systematically lower. We may make an adjustment to H_{sc2} by a factor 1.2 (we name these adjusted values H_{sca}), in order to make the values of H_{sca} similar to H_s. In this case also the periods of large difference between the predicted and observed wave height remain the same.

The periods when H_{sc1} of Fig. 7 and H_{sca} of Fig. 8 correspond to the measured H_s are common for both figures, and we can assume that in these periods the local equilibrium, as expressed by the form of Eq. (5a), was satisfied. Periods when there are big differences in the curves correspond, in case of STM24, to periods when the wind direction was changing drastically and local equilibrium is not to be expected. In the case of STM212 this was not necessarily the case (cf. Figs. 4 and 5). We assume that swell packets arrived during these periods of STM212, and we exclude those periods with horizontal arrows in Figs. 4–8 from the following analyses.

Within the periods when the analyses were made, there are still fluctuations in individual data points. However, we can consider that these fluctuations are intrinsic in wind and wind-wave fields. Toba et al. (1988) demonstrated that the wind-wave field takes some time (of the order of tens of minutes) to adjust itself to the fluctuation of wind. The local equilibrium expressed by Eq. (5a) holds only in a statistical sense. Thus, we exclude only the above-mentioned periods, when a systematic deviation both of H_{sc1} and H_{sca} with H_s exists. We consider that it is better to use a continuous series of data, that is as long as possible, instead of adopting a few discrete data points where local equilibrium is satisfied exactly. Also, in order to eliminate the short time fluctuations of wind and wind-wave field but to keep larger time-scale variations of wind and waves, three-point moving averaged time-series data, which means one-hour averaged data, will be used in the following sections.

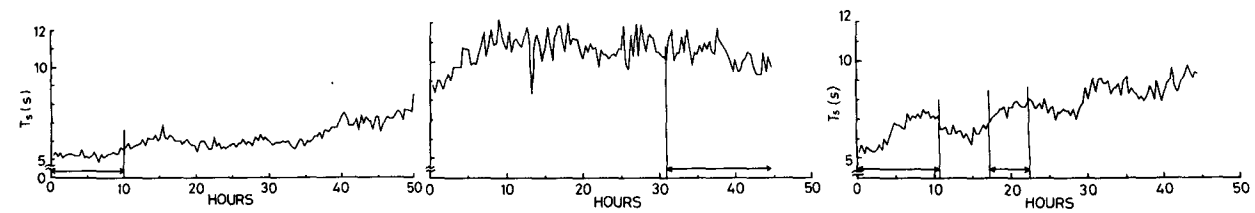

FIG. 6. Time series of significant wave period. Panels as in Fig. 4.

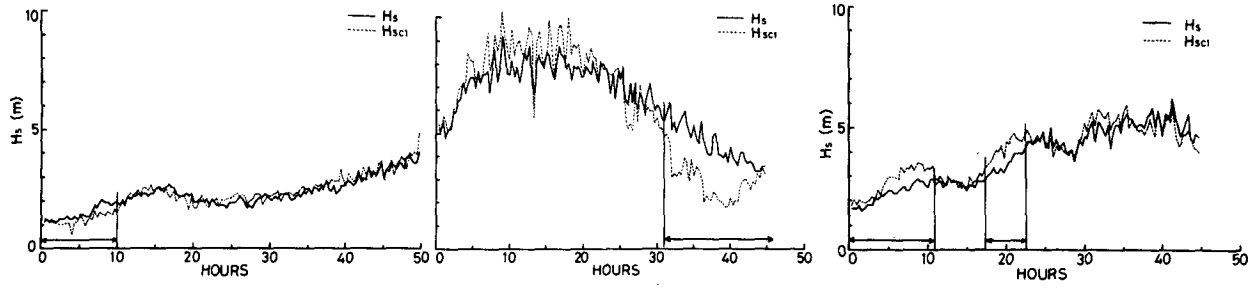

FIG. 7. Time series of significant wave height, H_s (thick line). Panels as in Fig. 4. The dotted line of H_{sc1} is the value calculated from wind speed and significant wave period by assuming Eqs. (3) and (14).

b. Preliminary considerations of the data satisfaction of the 3/2-power law (5a)

Excluding those portions indicated in Figs. 4–8 by horizontal arrows, we can generate two series of u_*, one assuming Charnock's expression, Eq. (1) and one assuming the new relation, Eq. (3), using the wind at one level and the logarithmic law Eq. (14). By using these two series of u_* together with the observed T_s and H_s, we examined the 3/2-power law. In the case where we used z_0 from Eq. (3), the value of $H_s/T_s^{3/2}$ has been plotted against $(gu_*)^{1/2}$ in Fig. 9. The closed circles are the Bass Strait data. The distribution of the Bass Strait data gives

$$B = 0.0603 \pm 0.0047, \qquad (15)$$

showing that the data points obey the 3/2-power law (5a) statistically. This value of B in Eq. (15) corresponds well to the value 0.062 which was proposed by Toba (1972). The figure also contains, for comparison, Shirahama Oceanographic Tower Station data by Kawai et al. (1977), for runs 9–26 where wind-waves prevailed, and lake measurements by Merzi and Graf (1985) and by Donelan (1979).

On the other hand, Fig. 10 shows the same Bass Strait data when Charnock's z_0 formula (1) was assumed. While in Fig. 9 all the data points were continuous, the Bass Strait points in Fig. 10 show an apparent disjoint with the other datasets, falling about a range of B that appears to be too large. In other words, the stratification of data in Fig. 10 was eliminated in Fig. 9 by assuming larger values of z_0 or of C_D given by Toba–Koga formula, instead of assuming traditional C_D values.

In Fig. 11, the same data of Bass Strait as Fig. 9 are plotted on a H^*–T^* diagram corresponding to Eq. (5). Since both H^* and T^* include u_*, the plot of Fig. 11 may include an effect of "spurious self-correlation" difficulty already discussed by Kenney (1982). Figure 9 presents the data in a dimensional form, corresponding to (5a), so that there is no variable common factor in both the ordinate and the abscissa.

In Eq. (5a), u_* appears in a form of $u_*^{1/2}$, or of $C_D{}^{1/4}$, since $u_* = (C_D)^{1/2}U_{10}$. The data points of Bass Strait in Fig. 10, which are distributed around $B = 0.062 + 20\%$ line, correspond to the average magnitude of C_D which is smaller by a factor of 2.1. It might be possible that one could make an adjustment of the value of β in Eq. (1) to collapse the data of Fig. 10. However, this requires a value of β which is twenty times larger than 0.0185 of Wu (1980), irrespective of the state of wind waves. Since in this case z_0 is a function only of u_*, this proposal of the large value of β should be rejected, as it is inconsistent with much previous data at low wave height.

4. Test of roughness expressions

Now that we have edited the data to include only local equilibrium waves and justified the choice of constant B in the 3/2-power law, we will test Eq. (1) and Eq. (3) in a more general way.

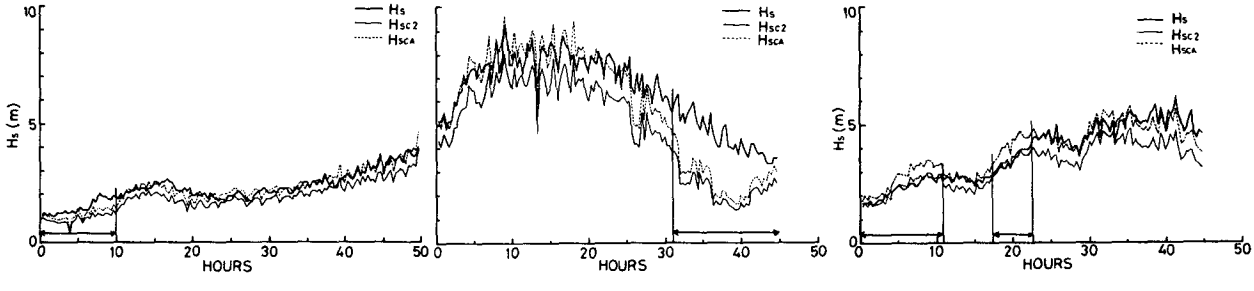

FIG. 8. As in Fig. 7 except for that the thin line of H_{sc2} is the value calculated from wind speed and significant wave period by assuming Eqs. (1) and (14), and that the dotted line of H_{sca} is the value obtained by the adjustment of H_{sc2} by a factor of 1.2.

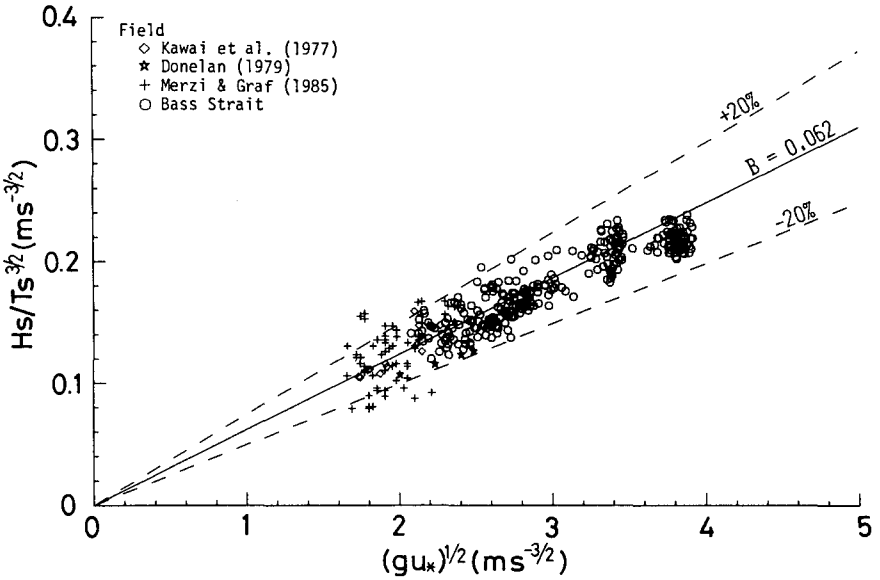

FIG. 9. Bass Strait data points showing the dimensional form of $^3/_2$-power law (open circles) together with Shirahama Oceanographic Tower Station data by Kawai et al. (1977), and lake measurements by Donelan (1979), Merzi and Graf (1985). For Bass Strait data, u_* was estimated by using Toba and Koga Eq. (3) and logarithmic profile (14).

We assume only the $^3/_2$-power law (5a) and the logarithmic wind profile (14) to obtain z_0 directly from the observed data. Namely, from the three-point moving averaged time-series values of H_s and T_s, we obtain u_* by using

$$u_* = H_s^2/B^2 g T_s^3, \quad B = 0.062, \qquad (16)$$

which follows from (5a). Then by using this u_* in the logarithmic law Eq. (14) together with the wind speed data, we can calculate z_0. The cloud of values of $z_0\sigma_p/u_*$ for Bass Strait are shown in Figs. 12 and 13, in which we have plotted the present data together with some representative data from laboratories and tower stations. For the measurements of Hsu et al. (1982) the value of z_0 was estimated by us from their published velocity profiles. For the data of Kunishi and Imasato (1966), Masuda and Kusaba (1987) those authors kindly supplied us with tables of z_0, u_* and σ_p.

Since the value of z_0 for aerodynamically smooth flow is determined only by u_* and the kinematic vis-

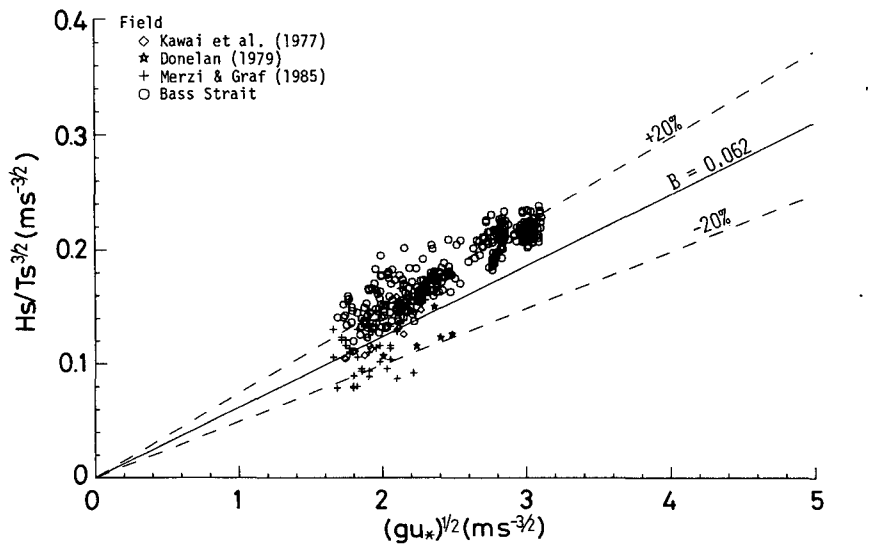

FIG. 10. As in Fig. 9 except that for Bass Strait data u_* was estimated by using Charnock's formula (1) and logarithmic profile (14). In this case stratification between Bass Strait data and other data is evident.

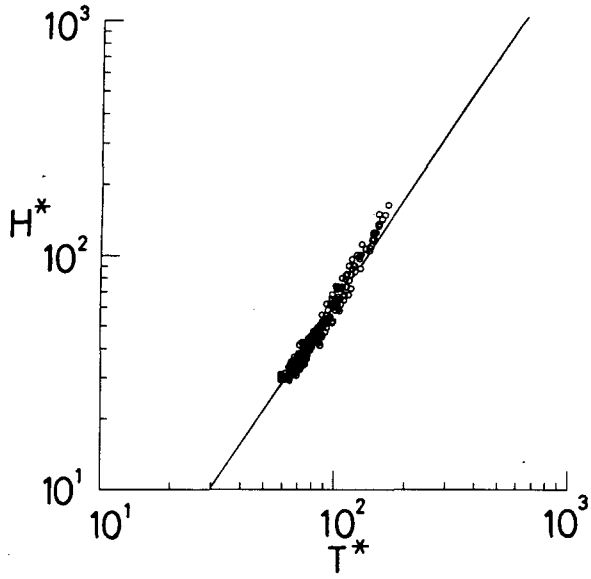

FIG. 11. Bass Strait data points showing the nondimensional $^3/_2$-power law (5).

cosity, ν, we restrict our attention to aerodynamically rough flows where, analogously to solid surface roughness criterion of Schlichting (1968), we use $u_* z_0/\nu > 2.3$. Since atmospheric stability also affects the value of z_0 we used only data where the Richardson number, defined in terms of the water temperature, T_w, and the air temperature at height z above the sea surface, T_a, in degrees Centigrade respectively, as

$$|\mathrm{Ri}| = |zg(T_a - T_w)/(273 + T_a)U^2| < 0.02. \quad (17)$$

For the Bass Strait data only T_a was directly available and T_w was obtained from the climatic averages presented in Jones (1980). It is noted that in all these data except the present Bass Strait data the values of z_0 were determined directly from wind profiles or flux measurements. The criteria for data acceptance are summarized in Table 1. It is evident that Eq. (3) holds statistically for a large range of T_s (Fig. 12), whereas the data points show a systematic deviation from Eq. (1) for larger values of T_s (Fig. 13).

The scattering of the data points here stems principally from the intrinsic fluctuation of the wind and wind-wave fields as seen in Figs. 5, 6 and 7 for the Bass Strait data. It should be noted also that, since z_0 appears in the logarithmic form in (14), the scattering of data of z_0 in the logarithmic diagram corresponds to the scattering of $(C_D)^{1/2}$ in a linear diagram, since $u_* = (C_D)^{1/2} U_{10}$. A variation in z_0 in two orders of magnitude corresponds to the variation in C_D only by a factor of about five.

It should also be noted that data by Merzi and Graf (1985) were taken at a tower station in Lake of Geneva in a water depth of 3 m, and they may be influenced by the shallow water depth. The Shirahama data by Kawai et al. (1977) was taken at a depth of 5–6 m, just at the critical depth for the shallow water effect.

Masuda and Kusaba (1987) proposed an expression:

$$gz_0/u_*^2 \propto (\sigma_p u_*/g)^{\epsilon}, \quad (18)$$

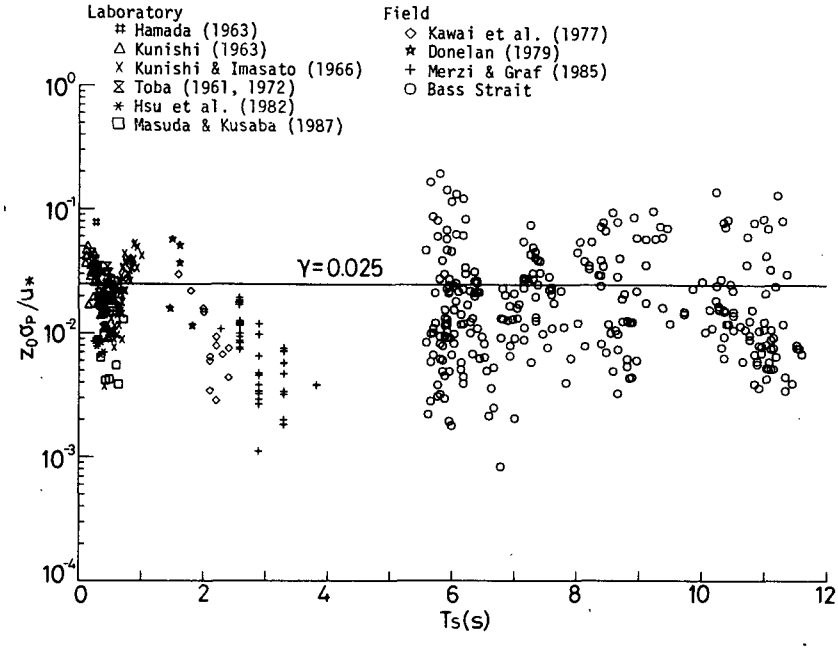

FIG. 12. Values of z_0 and u_*, obtained by assuming only the $^3/_2$-power law Eq. (5a) and the logarithmic law Eq. (14), show that Eq. (3) is statistically satisfied up to longer period wind waves.

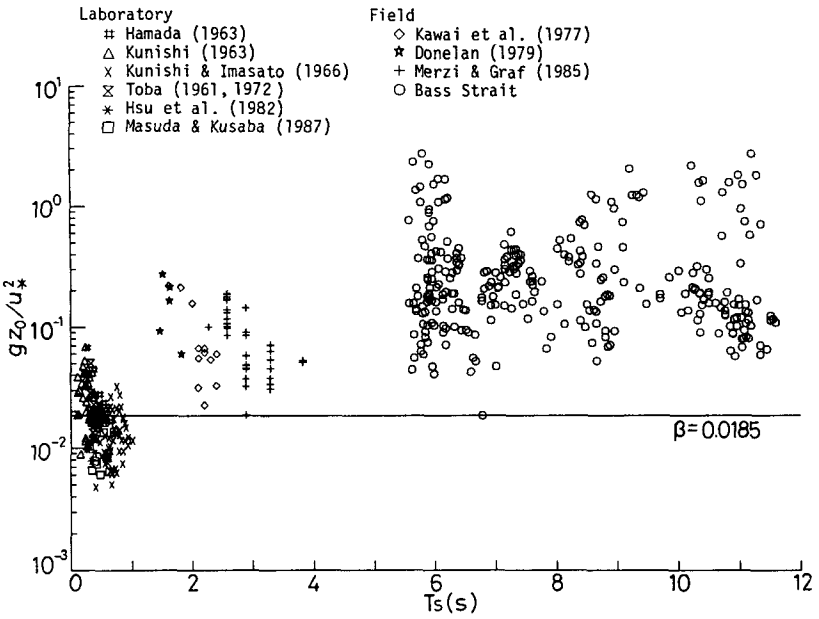

FIG. 13. The same data as in Fig. 12 do not satisfy Eq. (1) for longer period wind waves.

with ϵ as an exponent to be determined empirically. This is also one of the simple forms of Eq. (4). Charnock's expression (1) corresponds to $\epsilon = 0$ in this form, and our Eq. (3) to $\epsilon = -1$. Also, Hsu (1974) proposed another formula:

$$z_0 = H_s/2\pi(C_p/u_*)^2. \tag{19}$$

This formula can be rewritten, by using the $^3/_2$-power law (5), as

$$gz_0/u_*^2 = (2\pi)^{1/2}B(\sigma_p u_*/g)^{1/2}, \tag{20}$$

in which $\epsilon = {}^1/_2$. These are all particular examples of Eq. (4), a form for which Stewart (1974) in his review of a decade ago was unable to find much support from field data.

With the same data as in Figs. 12 and 13 we look again, in Fig. 14, at the empirical evidence for the form (18). The method of least squares applied to the composite dataset on the logarithmic scales gives

$$gz_0/u_*^2 = 0.0206(\sigma_p u_*/g)^{-0.842}. \tag{21}$$

This line is entered in Fig. 14 as a broken line. The composite dataset points thus support $\epsilon = -1$ which corresponds to Eq. (3), rather than $\epsilon = 0$ for Eq. (1). This contrasts with the value of ϵ which fitted the laboratory data presented by Masuda and Kusba (1987). Their data included a number of points that did not satisfy our criterion of aerodynamically rough and only those points that satisfied Table 1 were included in Figs. 12, 13 and 14. The lower limit of the abscissa for wind waves is entered by a vertical line at $\sigma_p u_*/g = 0.025$ or $C_p/u_* = 40$.

If we accept $\epsilon = -1$, the other constant γ for the present collection of data appears slightly lower than that estimated by Toba and Koga (1986), but we should await the collection of all relevant data before proposing a final value. The averaged value of γ for each dataset adopted for Figs. 12–14 is listed in Table 2, together with the whole dataset average value of γ. Since z_0 has a character to scatter on a logarithmic scale, the γ-values averaged on a logarithmic scale are also listed, which are naturally smaller than the linear-averaged values.

The present roughness length expression suggests values of C_D 2.1 times, on the average for these two Bass Strait storms, than that inferred from Charnock's expression. The sensitivity of the results to error in measurements needs to be examined. Equation (5a) can be rewritten as

$$C_D = g^{-2}U_{10}^{-2}H_s^4T_s^{-6}B^{-4}. \tag{22}$$

First, let us assume that the 2.1 times larger value of C_D comes from an error in the wind speed U_{10}. Since $C_D = u_*^2/U_{10}^2$, an error of $(2.1)^{1/2}$ or 45% is necessary in U_{10} to produce an error in C_D of a factor of 2.1. A measured wind speed of 22 m s^{-1} would need to be in reality 14 m s^{-1}. While the anemometer was given a cursory calibration monthly against a second ane-

TABLE 1. The criteria of data acceptance for Figs. 12, 13 and 14.

Equilibrium waves	$B = 0.062 \pm 20\%$
Near neutral	$\lvert Ri \rvert < 0.02$
Aerodynamically rough	$u_* z_0/\nu > 2.3$

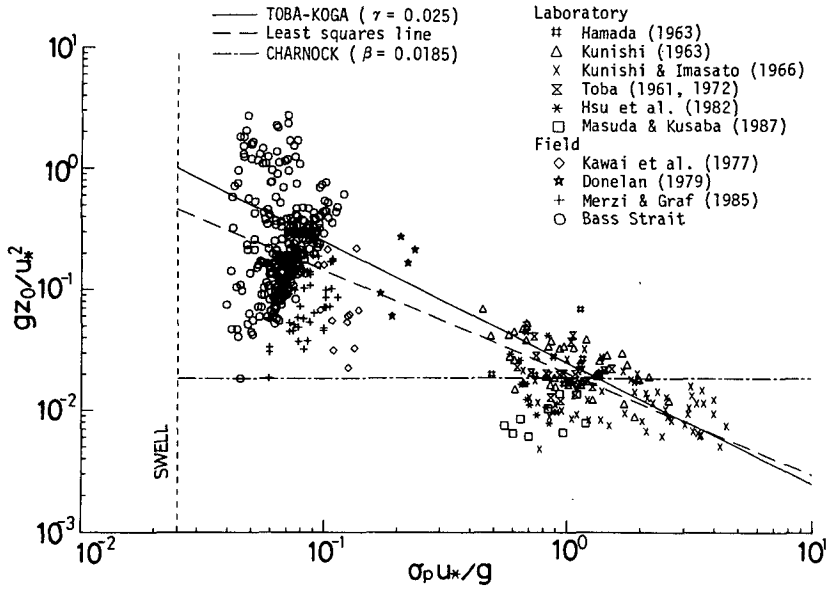

FIG. 14. The same data as in Figs. 12 and 13 indicating that the ϵ in Eq. (18) is close to -1. The full line indicates Toba–Koga formula Eq. (3), and the dash-dot line Charnock's formula Eq. (1). The broken line shows Eq. (21) in section 4 obtained by the method of least squares applied to the composite dataset. The vertical dotted line indicates $\sigma_p u_*/g = 0.025$ or $C_p/u_* = 40$, corresponding to the lower limit of the abscissa for wind waves.

mometer, there is some difficulty in assessing the error induced by flow distortion around the platform and the radio mast on which the anemometer was mounted. It was about 1 m from the lattice radio mast and for SE wind was beside rather than behind the radio mast. It was reported that an anemometer, mounted on a lattice tower with the distance of the order of the side of the tower, measured the wind speeds with an error of several percent except that there were large errors in the wind shadow arc of about 60° (Moses and Daubek 1961; Gill et al. 1967; Cermak and Horn 1968; Camp and Kaufman 1970). Also the marine boundary layer is likely to be accelerated by the platform itself and we would expect increased wind speed for SE flow at the position of the radio mast. It is difficult to estimate the magnitude of these changes. We doubt, however, that this could be as large as 45% though it may contribute somewhat to the high z_0. Next we assume an error in the measurement of H_s or T_s. Here we are on firmer ground. An error of $(2.1)^{-1/4}$ or -17% is necessary in H_s, or an error of $(2.1)^{1/6}$ or 13% is necessary in T_s to produce an error in C_D of a factor of 2.1. The wave height gauge was carefully calibrated monthly, and an intercomparison of the gauge used in this study with a sonic height gauge later in the Bass Strait series of experiments showed close agreement. Significant error in the digital calculations of wave height or period is not plausible (outside statistical fluctuations). Thus simple measurement error seems an unlikely cause for the large values of z_0 found from our present measurements.

5. Discussion

It has been shown that, for situations where the waves are in "local equilibrium with the wind," then, with the use of the $^3/_2$-power law of Eq. (16) to determine the stress u_*, we can test the relative merits of Charnock's expression Eq. (1) or our Eq. (3) for the roughness length z_0. The Bass Strait data supports Eq. (3), and Eq. (3) is consistent with earlier data where u_* was measured directly. The reasonable agreement found by some previous authors between their measured data and Charnock's expression may be due to grouping all types of wave fields together including both those in "local equilibrium with the wind" and those of greater wave age.

A physical interpretation of the existence of Eq. (3) may be given as follows. In a field of pure wind waves driven by a steady or slowly varying wind, there is a local equilibrium between the wind and the wind-wave field in a statistical sense, as expressed by the $^3/_2$-power law (5). This seems to hold in order to fulfill the constraints of the continuities between the air and water turbulent boundary layers, which are coupled together by the wind-waves. These constraints seem to be satisfied by the breaking adjustment of wind waves, resulting in the $^3/_2$-power law (Toba 1988). Then if the wind-wave field approaches a saturation state for infinite fetch (this state is expressed in Wilson's fetch graph formula (6a) by $\hat{H} = 0.30$), the momentum that entered to the wave field must go to the current in this state by wave breaking. This situation was expressed

(Toba 1978) by an error-functional form of the momentum retention factor G:

$$G = \tau^{-1} DM/Dt = 0.061\{1 - \mathrm{erf}(0.0073T^*)\} \quad (23)$$

where τ is the sea-surface wind stress, DM/Dt the rate of increase of the wind-wave momentum in the duration limited wave field; G becomes negligibly small as T^* ($=2\pi C_p/u_*$) becomes 250 or so. More wave momentum going to the current by the wave breaking produces more turbulent energy at the sea surface. Considering the constant wind U_{10}, it is thus expected that as the wave energy increases, the overall intensity of breaking and turbulence increases, and this in turn increases the momentum flux to the sea.

Another point of view is given as follows. The air and water turbulent boundary layers, expressed by the respective logarithmic velocity profile in a frame of reference moving with the interface velocity:

$$U(z)/u_* = (1/\kappa)\ln(z/z_0) \quad \text{for air} \quad (24)$$

$$-U(-z)/u_{*w} = (1/\kappa)\ln(-z/z_{0w}) \quad \text{for water} \quad (25)$$

and the wind-wave condition expressed by the $^3/_2$-power law, Eq. (5) together with Eq. (13):

$$gH_s/u_*^2 = B(2\pi g/1.05\sigma_p u_*)^{3/2}, \quad (26)$$

form a statistical local equilibrium by the mutual adjustment among wind waves, the air flow above and the water flow below the wind waves. The subscript w stands for the values in water corresponding to those in air. In this system of three equations, the approximate momentum flux continuity for steady state (i.e., negligible divergence of wave momentum flux) gives

$$u_{*w} = (\rho/\rho_w)^{1/2} u_*, \quad (27)$$

where ρ and ρ_w are densities of air and water, respectively. If we assume that z_{0w} is a unique function of z_0, or a similar assumption between C_{Dw} and C_D, the system of equations involves only four independent variables: z_0, σ_p (corresponding to T_s), g and u_*. Dimensional analysis of this system gives only two nondimensional variables. This situation corresponds to Eq. (4), and one example of how they can be related is Eq. (18).

Although Eqs. (18) or (4) are more general, the dataset of Fig. 14 suggests that $\epsilon = -1$, an expression in which g is not included. If g, which influences wind waves as in Eq. (26), did not effect the momentum transfer processes within the turbulent boundary layers directly, we could eliminate g from the system of variables important for the momentum flux. Then only three variables z_0, σ_p and u_* are left. By dimensional analysis, we have only one number: $z_0\sigma_p/u_*$ so that $\epsilon = -1$. This is not a function of any other variables, and consequently, it would be a universal constant. The data shows that its value is around 0.025 or a little smaller. The wave frequency σ_p appears in the nondimensional group by the reason that we already raised in the introduction. Also, wind waves are important in controlling the boundary layer turbulence, as Kawamura and Toba (1988) and Yoshikawa et al. (1988) demonstrated by the dependence on the wave phase of the characteristics of ordered motions in the boundary layer over and below wind waves.

In the present paper, we selected the cases where large "pure wind-waves" were developing. In a real sea, however, we often have remotely generated swells from various directions. These swells are not expected to have the same influence on z_0 as "local equilibrium waves." We should not use the angular frequency of the swell for Eq. (3). Experiments by Antonia and Chambers (1980) at the same site and Geernaert, et al. (1987) seem to include situations with swell present. Even though swells may be present, wind waves can coexist so long as the wind is blowing. We may be able to determine the wave energy and peak period of the wind driven part of the sea and use this in the z_0 determination, but the test of this hypothesis is left for the future.

From Eq. (3) and the logarithmic law (14) the value of C_D as a function of U_{10} and T_s can be derived (Toba and Koga 1986):

$$C_D = \kappa^2[\ln(2\pi z_{10}/\gamma) - \ln U_{10} - \ln T_s - 0.5\ln C_D]^{-2} \quad (28)$$

where z_{10} is 10 m and $\kappa = 0.4$. Eq. (28) can be solved by iteration, and the calculated values are shown for $\gamma = 0.015$ (see Table 2) in Fig. 15. We have included the line for aerodynamically smooth flow, and the criterion for full roughness. Since we are concerned with local equilibrium waves, the values of C_D for fixed H_s can also be shown as entered in Fig. 15.

However, the value of γ is not yet considered conclusive as mentioned before. Fig. 16 shows the case of

TABLE 2. Values of γ of Eq. (3) obtained from various datasets used in this study.

Dataset	Number of data points	γ-value averaged (Linear)	γ-value averaged (Logarithmic)
Laboratory			
Hamada (1963)	9	0.029	0.024
Kunishi (1963)	38	0.027	0.025
Kunishi & Imasato (1966)	56	0.025	0.022
Toba (1961, 1972)	23	0.023	0.021
Hsu et al. (1982)	12	0.012	0.011
Masuda & Kusaba (1987)	10	0.0088	0.0076
Field			
Kawai et al. (1977)	13	0.011	0.0083
Donelan (1979)	5	0.035	0.029
Merzi & Graf (1985)	43	0.0078	0.0064
Bass Strait	289	0.026	0.016
Whole dataset average	498	0.0230	0.0155

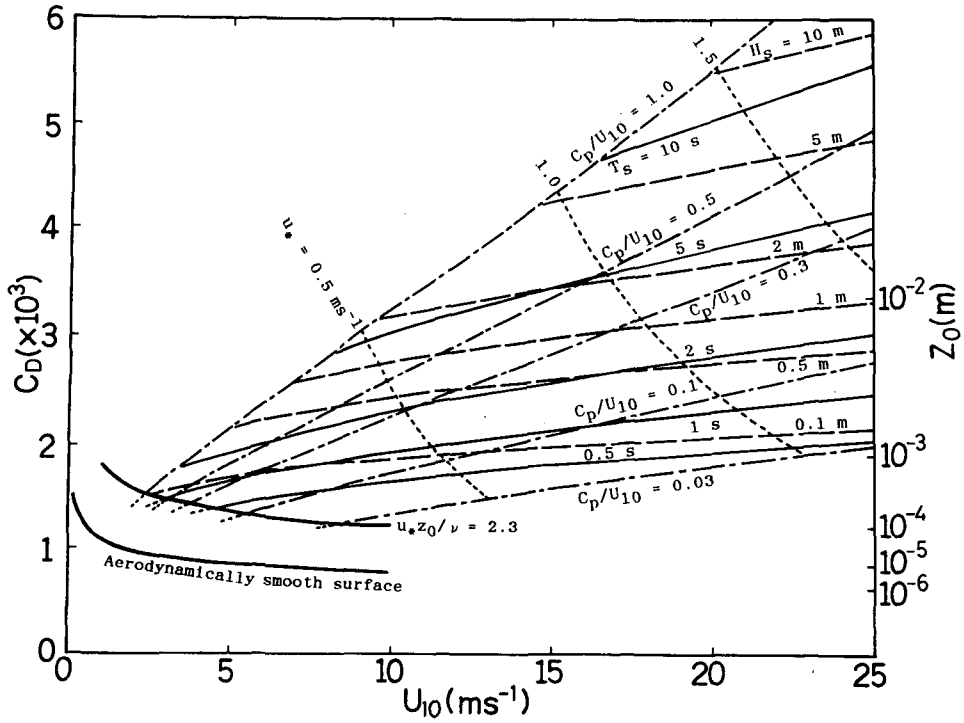

FIG. 15. Diagram for the drag coefficient C_D for a neutral stability atmosphere, as a function of U_{10} and T_s or H_s corresponding to Eq. (3) but with $\gamma = 0.015$ from Table 2, between the realistic wave age limits of $C_p/U_{10} = 0.03$ and 1.0.

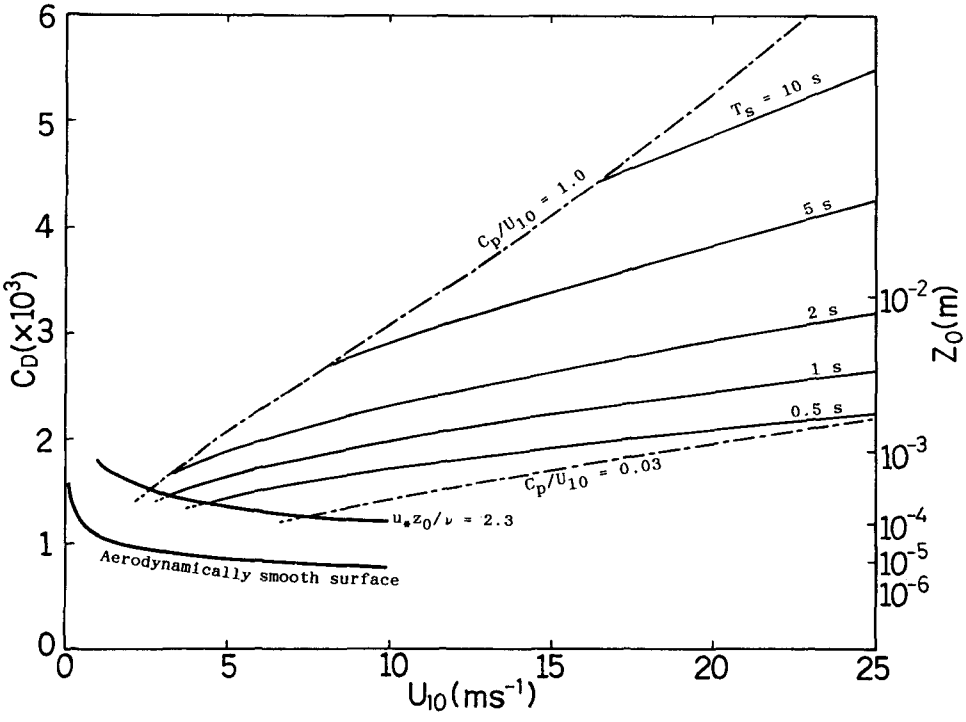

FIG. 16. Diagram for the drag coefficient for a neutral stability atmosphere, as a function of U_{10} and T_s corresponding to Eq. (21). Dash-dot lines indicate realistic wind-wave age limits.

Eq. (21). In this case no large difference is seen from the case of Fig. 15.

Also, since data points of Kawai et al. (1977), Merzi and Graf (1985) seem to lie between Eq. (1) and Eq. (3), there might be a possibility that we should consider another form which belongs to Eq. (4) or Eq. (18). Since the Bass Strait points have been obtained by using an indirect way in estimating z_0 and u_* as described in this article, we have attempted the application of the method of least squares to the composite dataset which excluded the Bass Strait points. This gives

$$gz_0/u_*^2 = 0.0189(\sigma_p u_*/g)^{-0.579}. \quad (29)$$

Since in this equation ϵ is closer to $-1/2$, a convenient value for analytical use, we have prepared Fig. 17, for a form

$$gz_0/u_*^2 = 0.020(\sigma_p u_*/g)^{-0.5}. \quad (30)$$

The value of the coefficient 0.020 was determined for a condition of the fixed exponent of -0.5. This predicts C_D two-times larger than Charnock for storm conditions.

Volkov (1970) and Geernaert et al. (1987) showed data which included swell, where C_D decreased with increasing C_p/u_*. If this relation is true, the data points would have to lie about line with the opposite slope to that in Fig. 14. In fact, we may also see such a tendency in the Bass Strait data points. However, over the sea, the variation of wind is usually more rapid than the variation of wave energy. As an extreme example, we can consider the case where the wind changes but the waves do not vary. Then, in the case of the above described procedure of analysis of the Bass Strait data, both u_* and z_0 vary in such a manner that points in Fig. 14 lie along lines tending from the lower left to the upper right. Also, there will be a possibility that nonlocal equilibrium conditions of wind waves, e.g., in the case of turning winds near atmospheric fronts, may change the stress regime itself. However, the trend of the whole dataset is that C_D becomes larger as wind waves develop, as already shown in Fig. 13.

Geernaert et al. (1986) analyzed data obtained in the North Sea and reported that the z_0-expression, including the wave age of component waves in the form of weighting function after Kitaigorodskii and Volkov (1965), was the best expression, when the phase speed of waves was modified for a shallow sea. It should be noted that Kitaigorodskii and Volkov expression has the tendency that z_0 becomes larger as the peak of the wave spectrum becomes of lower frequency.

The self-similarity spectral form for the high-frequency part of wind waves, which is consistent with the $3/2$-power law, was proposed by Toba (1973) as

$$\phi(\sigma) = \alpha_s g_* u_* \sigma^{-4}, \quad g_* = g(1 + Sk^2/\rho_w g), \quad (31)$$

where $\phi(\sigma)$ is one-dimensional frequency spectral density, S the surface tension, and k is wavenumber.

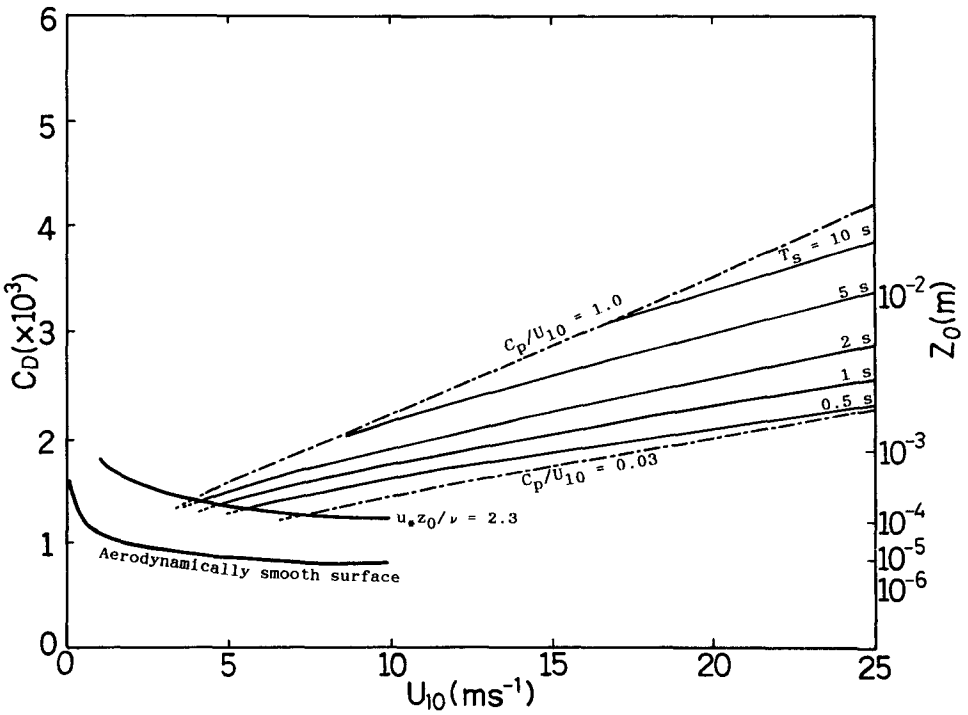

FIG. 17. As in Fig. 16 except for corresponding to Eq. (30).

Phillips (1985) and Battjes et al. (1987) have noted that the value of the constant α_s varies with investigator. One possible cause is that u_* is often estimated from U_{10} by using either a constant value of C_D or Charnock's formula (1). Too small values of u_* results in too large values of α_s. Consequently, there is a possibility that larger values of C_D, together with some other effects such as discussed in Toba et al. (1988) will solve the problem pointed out by Phillips (1985) of the inconsistency among proposed values of α_s.

If, as this paper suggests, the wind waves have a large effect on the value of C_D, then remote sensing of the ocean wind stress by satellite might be better carried out by measuring wave properties rather than the backscatter strength.

Also, if the bulk transfer coefficient for momentum, C_D, has this strong dependence on the character of the wind waves, other bulk transfer coefficients for heat, etc., can be expected to exhibit similar effects. This will also be an important subject to investigate. In fact, Kurasawa et al. (1983) analyzed the heat balance of the upper ocean south of Japan, by using data at the former Ocean Weather Station T, together with bulk formulas to estimate air–sea heat fluxes. According to their result, the heat convergence in the sea becomes negative around November (cf. their Table 1). This is not what is expected, since in this area of the sea the Kuroshio transports much heat and then transfers it into the atmosphere. The heat convergence in the sea should be positive all year round. This difficulty might be caused by Kurasawa et al. (1983), adopting too small values of the bulk transfer coefficients in the formulas for air–sea heat fluxes, especially for the winter monsoon season.

As a conclusion, we would say that, the results presented in this paper are consistent with one another in showing that in large growing windsea conditions C_D can be two to three times larger than the value that Charnock's expression usually predicts. Though Eq. (3) with $\gamma = 0.015$–0.025 should be applicable for pure wind-wave cases, a convenient conservative expression might be Eq. (30) for the windsea dependence of z_0. There are few datasets where both wind stress and simultaneous wave information are presented. Since the inferrence from the Bass Strait data has had some indirect elements, further experiments focussed on the wave dependence of the sea surface wind stress are to be encouraged.

Acknowledgments. We wish to thank ESSO-BHP for allowing us to make measurements over a number of years from their Bass Strait platforms. We also express our many thanks to various colleagues: Professor Robert W. Stewart and Professor Klaus Hasselmann took much time for valuable discussion. Professor N. Imasato and Dr. A. Masuda kindly provided us with their numerical data of wind-wave tank experiment. Professor J. Wu gave us comments at the first stage of our manuscript. We thank also to Mr. G. Yamanaka and Misses J. Kamata and A. Kikuta for their assistance in this research. This study was partially supported by a Grant-in-Aid for Scientific Research by the Japanese Ministry of Education, Science and Culture (Monbusho), and also by a grant under a Monbusho International Scientific Research Program.

REFERENCES

Antonia, R. A., and A. J. Chambers, 1980: Wind-wave-induced disturbances in the marine surface layer. *J. Phys. Oceanogr.*, **10,** 611–622.

Bailey, R. J., I. S. F. Jones and Y. Toba, 1989: The steepness and shape of wind waves. *J. Oceanogr. Soc. Japan,* submitted.

Banner, M. L., and W. K. Melville, 1976: On the separation of air flow over water waves. *J. Fluid Mech.*, **77,** 825–842.

Battjes, J. A., T. J. Zitman and L. H. Holthuijsen, 1987: A reanalysis of the spectra observed in JONSWAP. *J. Phys. Oceanogr.*, **17,** 1288–1295.

Blanc, T. V., 1983: Typical influences of moisture on profile measurements in the marine atmospheric surface layer. *Bound.-Layer Meteor.*, **25,** 411–415.

——, 1985: Variation of bulk-derived surface flux, stability, and roughness results due to the use of different transfer coefficient schemes. *J. Phys. Oceanogr.*, **15,** 650–669.

Boyle, P. J., K. L. Davidson and D. E. Spiel, 1987: Characteristics of over water surface stress during STREX. *Dyn. Atmos. Oceans,* **10,** 343–358.

Brutsaert, W., and Y. Toba, 1986: A quasi-similarity between wind waves and solid surfaces in their roughness characteristics. *J. Oceanogr. Soc. Japan,* **42,** 166–173.

Camp, D. W., and J. W. Kaufman, 1970: Comparison of tower influence on wind velocity for NASA's 150-meter meteorological tower and a wind tunnel model of the tower. *J. Geophys. Res.*, **75,** 1117–1121.

Cermak, J. E., and J. D. Horn, 1968: Tower shadow effect. *J. Geophys. Res.*, **73,** 1869–1876.

Charnock, H., 1955: Wind stress on a water surface. *Quart. J. Roy. Meteor. Soc.*, **81,** 639–640.

Donelan, M. A., 1979: On the fraction of wind momentum retained by waves. *Marine Forecasting,* J. C. J. Nihoul, Ed., Elsevier, 141–159.

——, 1982: The dependence of the aerodynamic drag coefficient on wave parameters. *Proc. First Int. Conf. on Meteor. and Air–Sea Interaction of the Coastal Zone,* The Hague, Amer. Meteor. Soc., 381–387.

Garratt, J. R., 1977: Review of drag coefficients over oceans and continents. *Mon. Wea. Rev.*, **105,** 915–929.

Geernaert, G. L., K. B. Katsaros and K. Richter, 1986: Variation of the drag coefficient and its dependence on sea state. *J. Geophys. Res.*, **91,** 7667–7679.

——, S. E. Larsen and F. Hansen, 1987: Measurements of the wind stress, heat flux, and turbulence intensity during storm conditions over the North Sea. *J. Geophys. Res.*, **92,** 13 127–13 139.

Gill, G. C., L. E. Olsson, J. Sela and M. Suda, 1967: Accuracy of wind measurements on towers or stacks. *Bull. Amer. Meteor. Soc.*, **48,** 665–674.

Hamada, T., 1963: An experimental study of development of wind waves. Rep. Port and Harbour Tech. Res. Inst., No. 2, 1–41.

Hasselmann, K., T. P. Barnett, E. Bouws, H. Carlson, D. E. Cartwright, K. Enke, J. A. Ewing, H. Gienapp, D. E. Hasselmann, P. Kruseman, A. Meerburg, P. Muller, D. J. Olbers, K. Richter, W. Sell and H. Walden, 1973: Measurements of wind-wave growth and swell decay during the Joint North Sea Wave Project (JONSWAP). *Dtsch. Hydrogr. Z.*, **8**(Suppl), 1–95.

Hsu, C., H. Wu, E. Hsu and R. L. Smith, 1982: Momentum and energy transfer in wind generated waves. *J. Phys. Oceanogr.*, **12,** 929–951.

Hsu, S. A., 1974: A dynamic roughness equation and its application to wind stress determination at the air-sea interface. *J. Phys. Oceanogr.*, **4**, 116–120.

Jones, I. S. F., 1980: Tidal and wind-driven currents in Bass Strait. *Aust. J. Mar. Freshwater Res.*, **31**, 109.

——, and Y. Toba, 1985: Wave data from three Bass Strait Storms. Marine Studies Centre Tech. Rep., The Univ. of Sydney, **2/85**, 30 pp.

Kawai, S., K. Okada and Y. Toba, 1977: Support of the $^3/_2$-power law and the $gu_*\sigma^{-4}$-spectral form for growing wind waves with field observational data. *J. Oceanogr. Soc. Japan*, **33**, 137–150.

Kawamura, H., and Y. Toba, 1988: Ordered motion in the turbulent boundary layer over wind waves. *J. Fluid Mech.*, **197**, 105–138.

Kenney, B. C., 1982: Beware of spurious self-correlations! *Water Resour. Res.*, **18**, 1041–1048.

Kitaigorodskii, S. A., and Yu. A. Volkov, 1965: On the roughness parameter of the sea surface and the calculation of momentum flux in the near-water layer of the atomsphere. *Izv. Atmos. Ocean. Phys.*, **1**, 973–988.

——, and M. M. Zaslavsky, 1974: A dynamical analysis of the drag conditions at the sea surface. *Bound.-Layer Meteor.*, **6**, 53–61.

Kondo, J., 1975: Air-sea bulk transfer coefficients in diabatic conditions. *Bound.-Layer Meteor.*, **9**, 91–112.

——, Y. Fujinawa and G. Naito, 1973: High-frequency components of ocean waves and their relation to the aerodynamic roughness. *J. Phys. Oceanogr.*, **3**, 197–202.

Kunishi, H., 1963: An experimental study on the generation and growth of wind waves. Disaster Prevention Res. Inst., Kyoto University, Bull., No. 61, 41 pp.

——, and N. Imasato, 1966: On the growth of wind waves in high-speed wind flume. Annuals, Disast. Prev. Res. Inst., Kyoto Univ., **9**, 667–676. (in Japanese with Eng. Abstr.)

Kurasawa, Y., K. Hanawa and Y. Toba, 1983: Heat balance of the surface layer of the sea at Ocean Weather Station T. *J. Oceanogr. Soc. Japan*, **39**, 192–202.

Masuda, A., and T. Kusaba, 1987: On the local equilibrium of winds and wind-waves in relation to surface drag. *J. Oceanogr. Soc. Japan*, **43**, 28–36.

Melville, W. K., 1977: Wind stress and surface roughness over breaking waves. *J. Phys. Oceanogr.*, **7**, 702–710.

Merzi, N., and W. H. Graf, 1985: Evaluation of the drag coefficient considering the effects of mobility of the roughness elements. *Ann. Geophys.*, **3**, 473–478.

Mitsuyasu, H., 1968: On the growth of the spectrum of wind-generated waves (I). Rep. Res. Inst. Appl. Mech., Kyushu Univ., **16**, 459–482.

——, R. Nakamura and T. Komori, 1971: Observation of the wind and waves in Hakata Bay. Rep. Res. Inst. Appl. Mech., Kyushu Univ., **19**, 37–74.

Moses, H., and H. G. Daubek, 1961: Errors in wind measurements associated with tower-mounted anemometers. *Bull. Amer. Meteor. Soc.*, **42**, 190–194.

Phillips, O. M., 1985: Spectral and statistical properties of the equilibrium range in wind-generated gravity waves. *J. Fluid Mech.*, **156**, 505–531.

Schlichting, H., 1968: *Boundary-Layer Theory.* McGraw-Hill, pp 747.

Smith, S. D., and E. G. Banke, 1975: Variation of the sea surface drag coefficient with wind speed. *Quart. J. Roy. Meteor. Soc.*, **101**, 665–673.

Stewart, R. W., 1974: The air–sea momentum exchange. *Bound.-Layer Meteor.*, **6**, 151–167.

Toba, Y., 1961: Drop production by bursting of air bubbles on the sea surface (III). Study by use of a wind flume. *Mem. Coll. Sci., Univ. of Kyoto*, Ser. A, **29**, 313–344.

——, 1972: Local balance in the air–sea boundary processes. I. On the growth process of wind waves. *J. Oceanogr. Soc. Japan*, **28**, 109–120.

——, 1973: Local balance in the air–sea boundary processes. III. On the spectrum of wind waves. *J. Oceanogr. Soc. Japan*, **29**, 209–220.

——, 1978: Stochastic form of the growth of wind waves in a single-parameter representation with physical implications. *J. Phys. Oceanogr.*, **8**, 494–507.

——, 1979: Study on wind waves as a strongly nonlinear phenomenon. *Twelfth Symp. on Naval Hydrodynamics*, Natl. Acad. of Sci., Washington, DC, 529–540.

——, 1985: Wind waves and turbulence. *Recent Studies of Turbulent Phenomena*, T. Tatsumi, H. Maruo and H. Takami, Eds., Assoc. for Sci. Doc., Tokyo, 277–296.

——, 1988: Similarity laws of the wind wave and the coupling process of the air and water turbulent boundary layers. *Fluid Dyn. Res.*, **2**, 263–279.

——, and H. Kunishi, 1970: Breaking of wind waves and the sea surface wind stress. *J. Oceanogr. Soc. Japan*, **26**, 71–80.

——, and M. Koga, 1986: A parameter describing overall conditions of wave breaking, whitecapping, sea-spray production and wind stress. *Oceanic Whitecaps*, E. C. Monahan and G. Mac Niocaill, Eds., D. Reidel, 37–47.

——, S. Kawai and P. S. Joseph, 1985: The TOHOKU Wave Model. *Ocean Wave Modeling*, The SWAMP Group, Plenum, 201–210.

——, K. Okada and I. S. F. Jones, 1988: The response of wind-wave spectra to changing winds. I. Increasing winds. *J. Phys. Oceanogr.*, **18**, 1231–1240.

Volkov, Yu. A., 1970: Turbulent flux of momentum and heat in the atmospheric surface layer over a disturbed sea-surface. *Isv., Atmos. Ocean. Phys.*, **6**, 1295–1302.

Wilson, B. W., 1965: Numerical perdiction of ocean waves in the North Atlantic for December. *Dtsch. Hydrogr.*, **18**, 114–130.

Wu, J., 1980: Wind-stress coefficients over sea surface near neutral conditions—A revisit. *J. Phys. Oceanogr.*, **10**, 727–740.

——, 1986: Roughness elements of the sea-surface—Their spectral composition. *Tellus*, **38A**, 178–188.

——, 1988: On nondimensional correlation between roughness length and wind-friction velocity. *J. Oceanogr. Soc. Japan*, **44**, 254–260.

Yoshikawa, I., H. Kawamura, K. Okuda and Y. Toba, 1988: Turbulent structure in water under laboratory wind waves. *J. Oceanogr. Soc. Japan*, **44**, 143–156.